

H₂O Maser Pumping: The Effect of Quasi-Resonance Energy Transfer in Collisions between H₂ and H₂O Molecules

A.V. Nesterenok ^{1*} and D.A. Varshalovich ^{1,2}

¹ Ioffe Physical-Technical Institute, Politekhnicheskaya St. 26, Saint Petersburg, 194021 Russia

² St. Petersburg State Polytechnical University, Politekhnicheskaya St. 29, Saint Petersburg, 195251 Russia

* e-mail: alex-n10@yandex.ru

Abstract

The effect of quasi-resonance energy transfer in collisions between H₂ and H₂O molecules in H₂O maser sources is investigated. New data on the state-to-state rate coefficients for collisional transitions for H₂O and H₂ molecules are used in the calculations. The results of ortho-H₂O level population inversion calculations for the 22.2-, 380-, 439-, and 621-GHz transitions are presented. The ortho-H₂O level population inversion is shown to depend significantly on the population distribution of the para-H₂ $J = 0$ and 2 rotational levels. The possibility of quasi-resonance energy transfer in collisions between H₂ molecules at highly excited rotational-vibrational levels and H₂O molecules is considered. The quasi-resonance energy transfer effect can play a significant role in pumping H₂O masers in the central regions of active galactic nuclei and in star-forming regions.

Keywords: *cosmic masers, star-forming regions, active galactic nuclei.*

DOI: 10.1134/S1063773714070068

Introduction

H₂O maser emission is observed in many astrophysical objects: in the expanding envelopes of late-type stars, star-forming regions, and the central regions of active galactic nuclei (AGNs). The isotropic luminosities in the 22.2-GHz line for sources observed in our Galaxy lie between $\lesssim 10^{-7}$ and $10^{-2} L_{\odot}$, reaching $1 L_{\odot}$ in rare cases (W49N) (Palagi et al. 1993; Liljeström et al. 1989). The brightest Galactic H₂O masers are observed in star-forming regions. H₂O maser emission in star-forming regions is generated in circumstellar disks and the shocks produced by bipolar outflows and stellar winds from young stars (Torrelles et al. 2005).

The first 22.2-GHz H₂O maser sources discovered in other galaxies had isotropic luminosities of 0.1–1 L_{\odot} (Churchwell et al. 1977). In 1979, however, dos Santos and Lépine (1979) detected intense H₂O maser emission from the central region of the galaxy NGC 4945. The isotropic luminosity of the maser was $\sim 100 L_{\odot}$, which is higher than the typical luminosities of H₂O maser sources in our Galaxy by several orders of magnitude. About 150 galaxies with intense H₂O maser emission observed from their central regions are known at present (Tarchi 2012). The isotropic luminosities of the sources in specific cases exceed $10^4 L_{\odot}$ (Castangia et al. 2011). All these galaxies have evidence of activity in the galactic nuclei. H₂O maser emission in the central regions of AGNs is generated in accretion disks around supermassive black holes (Moran 2008). In specific cases, H₂O maser emission can be observed along the radio jet (Peck et al. 2003) and can be associated with the outflows of dense molecular gas from the central engine (Greenhill et al. 2003). H₂O maser emission is a unique tool for investigating the structure and kinematics of the gas in the neighbourhoods of the central engines in AGNs.

As a rule, the collisional excitation of H₂O molecules to higher lying levels followed by the radiative de-excitation of these levels is considered as the main H₂O-maser pumping mechanism (Strelnitskii 1973; Yates et al. 1997). Varshalovich et al. (1983) proposed an H₂O-maser pumping mechanism in which the H₂O levels are excited through quasi-resonance energy transfer in collisions between H₂ and H₂O molecules. The absorption of ultraviolet radiation, the collisions of molecules with high-energy

photoelectrons, and formation reactions lead to the population of highly excited rotational-vibrational molecular levels. The listed processes can take place in photo- and X-ray dissociation regions as well as in dissociative shocks. The de-excitation of excited molecular levels can occur both through the emission of electromagnetic radiation and through collisional processes. The quasi-resonance excitation energy transfer in collisions between molecules is possible.

In this paper, we investigate the effect of quasi-resonance energy transfer in collisions between H_2 and H_2O molecules on the H_2O level population inversion. The collisional rate coefficients from Dubernet et al. (2009) and Daniel et al. (2010, 2011) were used. In our calculations, we took into account the state-to-state collisional transitions for the lower 45 ortho- H_2O rotational levels and the para- H_2 $J = 0$ and 2 levels. The simple model of a gas-dust cloud with constant physical parameters was considered. In our calculations of level populations, we used the accelerated Λ -iteration method (Rybicki and Hummer 1991).

Quasi-resonance Energy Transfer in Collisions between H_2O and H_2 Molecules

The main quasi-resonance conditions in collisions between molecules are: the Massey criterion, the conservation of the particle total rotational angular momentum, the conservation of the product of the parities of the particle wave functions, and the nuclear spin conservation for each of the molecule (Varshalovich et al. 1983).

According to the Massey criterion, the increment in the sum of the excitation energies of the molecules before and after their collision must satisfy the inequality $|\Delta\varepsilon| \lesssim \hbar v/\rho$, where $|\Delta\varepsilon|$ is the excitation energy defect, v is the relative velocity of the particles, and ρ is their characteristic interaction radius. For collisions between H_2O and H_2 , this condition can be rewritten as

$$|\Delta\varepsilon| \lesssim \frac{\hbar v_T}{\rho} \simeq 4 \times 10^{-16} \sqrt{T_g} \text{ erg}, \quad (1)$$

where v_T is the mean relative velocity of the molecules, T_g is the kinetic temperature of the gas in kelvins; in our estimation, the H_2O - H_2 interaction radius ρ was assumed to be 2.5\AA (Valiron et al. 2008). The excitation energy defect is

$$\Delta\varepsilon = \varepsilon_{\text{H}_2\text{O}} + \varepsilon_{\text{H}_2} - \varepsilon'_{\text{H}_2\text{O}} - \varepsilon'_{\text{H}_2},$$

where ε and ε' are the level energies of the molecules before and after their collision, respectively.

The conditions for the conservation of the total angular momentum of the molecules and the conservation of the product of the parities can be written as (Varshalovich et al. 1983)

$$\mathbf{J}_{\text{H}_2} + \mathbf{J}_{\text{H}_2\text{O}} = \mathbf{J}'_{\text{H}_2} + \mathbf{J}'_{\text{H}_2\text{O}}, \quad \pi_{\text{H}_2}\pi_{\text{H}_2\text{O}} = \pi'_{\text{H}_2}\pi'_{\text{H}_2\text{O}}, \quad (2)$$

where \mathbf{J} and \mathbf{J}' are the rotational angular momentum vectors of the molecule before and after the collision, π and π' are the parities of the molecule's wave function with respect to spatial coordinate inversion before and after the collision, respectively (the change of orbital angular momentum of the relative motion of the molecules in this case is 0). The parity of the wave functions is $\pi_{\text{H}_2} = (-1)^J$ for the H_2 molecule and $\pi_{\text{H}_2\text{O}} = (-1)^{J+K_a+K_c}$ for the H_2O molecule, where K_a and K_c are the quantum numbers that characterize the projections of the rotational angular momentum vector onto the molecule's internal axes (Tennyson et al. 2001). The nuclear spin conservation for the molecules means that the transitions changing the ortho/para states of the molecules are forbidden:

$$I_{\text{H}_2\text{O}} = I'_{\text{H}_2\text{O}}, \quad I_{\text{H}_2} = I'_{\text{H}_2}, \quad (3)$$

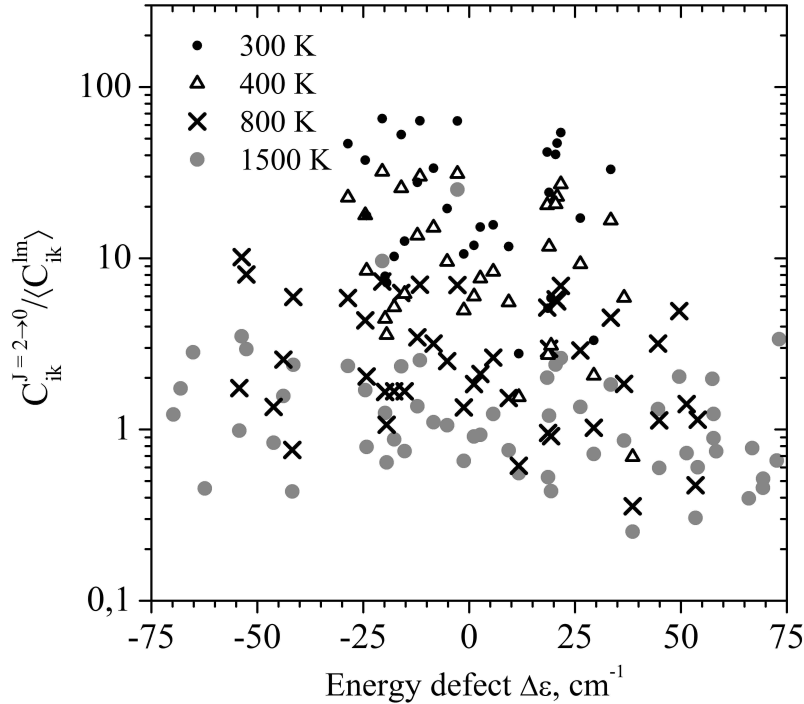


Figure 1: Ratios of the collisional rate coefficients for the H₂O and H₂ transitions for which quasi-resonance energy transfer takes place and their mean values for the transitions without any quasi-resonance. The excitation energy defect is along the horizontal axis. The data are presented for four temperatures (300, 400, 800, and 1500 K).

where I and I' are the nuclear spins of the molecules before and after their collision, $I = 0$ and 1 correspond to the para- and ortho-states, respectively.

Dubernet et al. (2009) provide the rate coefficients for transitions in collisions between ortho-H₂O and para-H₂ molecules for the lower 45 H₂O rotational levels and for H₂ in the $J = 0$ state with the change in rotational angular momentum $\Delta J = 0, +2$ as well as for H₂ in the $J = 2$ state with $\Delta J = 0, -2$. Consider the collisional H₂O transitions from level i to level k and the H₂ transitions from the $J = 2$ level to the $J = 0$ level, for which the quasi-resonance conditions (1)-(3) are met. We will denote the corresponding collisional rate coefficients by $C_{ik}^{J=2 \rightarrow 0}$, with $i < k$. Figure 1 presents the ratios of the collisional rate coefficients for quasi-resonance H₂O excitation and their mean values for the transitions without any quasi-resonance, i.e., $C_{ik}^{J=2 \rightarrow 0} / \langle C_{ik}^{lm} \rangle$. The averaging in $\langle C_{ik}^{lm} \rangle$ is performed over the following $l \rightarrow m$ transitions in H₂: $J = 0 \rightarrow 0, 0 \rightarrow 2, 2 \rightarrow 2$. The mean ratios of the rate coefficients are approximately 27, 13, 3, and 2 for gas temperatures of 300, 400, 800, and 1500 K, respectively.

Model Parameters

The observed sizes of H₂O maser sources in star-forming regions are $\sim 10^{12} - 10^{13}$ cm (Matveyenko et al. 2000; Uscanga et al. 2005; Matveyenko and Demichev 2010). To all appearances, the sizes of maser sources in accretion disks in the central regions of AGNs are $\sim 10^{14}$ cm (Kartje et al. 1999). The gas densities in H₂O maser sources can lie within the range $10^7 - 10^{10}$ cm⁻³. At higher densities, there is thermalization of the level populations due to collisional processes. To all appearances, lower gas densities are also unlikely, because a high relative H₂O abundance is needed in this case. High H₂O column densities along the line of sight, $10^{18} - 10^{19}$ cm⁻², are needed for the generation of intense H₂O maser emission

(Yates et al. 1997). The gas temperature in maser sources is 300-1500 K. At higher temperatures, there is dissociation of H₂O molecules (Nesterenok and Varshalovich 2011). The collisional maser pumping is most efficient when the dust temperature is much lower than the gas temperature (Bolgova et al. 1977; Yates et al. 1997; Babkovskaia and Poutanen 2004).

Here, we consider a one-dimensional plane parallel gas-dust cloud structure. The cloud sizes along two coordinate axes are much larger than that along the third z coordinate axis. As a rule, the model of a flat cloud is considered for modeling the H₂O maser emission in the envelopes of late-type stars and in star-forming regions (Nesterenok et al. 2013; Hollenbach et al. 2013).

The physical parameters adopted in our calculations are given in the table.

Table

Cloud half-thickness	$H = 10^{13}$ cm
Total number density of hydrogen atoms	$10^7 \text{ cm}^{-3} \leq N_{\text{H,tot}} \leq 10^{10} \text{ cm}^{-3}$
Ratio of H ₂ and H number densities	$N_{\text{H}_2}/N_{\text{H}} = 1$
Relative He abundance	$N_{\text{He}}/N_{\text{H,tot}} = 0.1$
Number density of ortho-H ₂ O molecules	$N_{\text{H}_2\text{O}} = 5 \times 10^4 \text{ cm}^{-3}$
Ortho-H ₂ O column density (perpendicular to cloud plane)	$\mathcal{N}_{\text{H}_2\text{O}} = 2HN_{\text{H}_2\text{O}} = 10^{18} \text{ cm}^{-2}$
Gas temperature	$300 \text{ K} \leq T_g \leq 1500 \text{ K}$
Dust temperature	$T_d = 100 \text{ K}$
Turbulent velocity	$v_{\text{turb}} = 1 \text{ km s}^{-1}$

The total number density of hydrogen atoms is $N_{\text{H,tot}} = N_{\text{H}} + 2N_{\text{H}_2}$

Calculating the H₂O Level Populations in a Gas-Dust Cloud

Radiative Transfer in Molecular Lines

We consider a gas-dust cloud that consists of a mixture of H₂ and H₂O molecules, H and He atoms, and dust particles. The physical parameters (the number densities of atoms and molecules, the dust content, the gas and dust temperatures) are assumed to be independent of the coordinates. However, the H₂O level populations are considered as functions of the z coordinate.

In the one-dimensional geometry, the intensity of radiation I at frequency ν depends on depth z and angle θ between the z axis and the radiation direction. The quantity $\mu = \cos\theta$ is used instead of the variable angle θ . The radiative transfer equation can be written as

$$\mu \frac{dI(z, \mu, \nu)}{dz} = -\kappa(z, \nu)I(z, \mu, \nu) + \varepsilon(z, \nu), \quad (4)$$

where $I(z, \mu, \nu)$ is the intensity of radiation at frequency ν in direction μ , $\varepsilon(z, \nu)$ is the emission coefficient, and $\kappa(z, \nu)$ is the absorption coefficient. The point $z = 0$ corresponds to the cloud boundary and the z axis is directed into the cloud. The boundary condition for Eq. (4) at $z = 0$ is $I(0, \mu, \nu) = 0$, where $\mu > 0$ (the directions into the cloud). At $z = H$, the boundary condition is taken to be $dI(z = H, \mu, \nu)/dz = 0$, corresponding to a cloud symmetric in physical parameters relative to $z = H$. Thus, the total cloud thickness is $2H$.

Each of the coefficients $\varepsilon(z, \nu)$ and $\kappa(z, \nu)$ is the sum of the emission or absorption coefficient in continuum and the emission or absorption coefficient in a spectral line, respectively:

$$\begin{aligned}\varepsilon(z, \nu) &= \varepsilon_c(\nu) + \frac{h\nu}{4\pi} A_{ik} N n_i(z) \phi_{ik}(\nu), \\ \kappa(z, \nu) &= \kappa_c(\nu) + \frac{\lambda^2}{8\pi} A_{ik} N \left(\frac{g_i}{g_k} n_k(z) - n_i(z) \right) \phi_{ik}(\nu).\end{aligned}$$

Here, $\varepsilon_c(\nu)$ and $\kappa_c(\nu)$ are the dust emission and absorption coefficients in continuum, respectively; A_{ik} is the Einstein coefficient for spontaneous emission; $n_i(z)$ and $n_k(z)$ are the normalized populations of levels i and k , $\sum_j n_j(z) = 1$; N is the particle number density; g_i and g_k are the statistical weights of the levels; λ is the radiation wavelength; and $\phi_{ik}(\nu)$ is the normalized spectral line profile. In these formulas, it is implied that level i lies above level k in energy, i.e., $\varepsilon_i > \varepsilon_k$. The spectral profile of the emission and absorption coefficients $\phi_{ik}(\nu)$ is

$$\phi_{ik}(\nu) = \frac{1}{\sqrt{\pi} \Delta\nu_{ik}} \exp\left(-\left(\frac{\nu - \nu_{ik}}{\Delta\nu_{ik}}\right)^2\right),$$

where ν_{ik} is the transition frequency and $\Delta\nu_{ik}$ is the line profile width. The line profile width is determined by the spread in thermal velocities of the molecules and turbulent velocities in the gas-dust cloud:

$$\Delta\nu_{ik} = \nu_{ik} \frac{v_D}{c}, \quad v_D^2 = v_T^2 + v_{\text{turb}}^2,$$

where $v_T = \sqrt{2kT_g/m}$ is the most probable thermal velocity of the molecules, k is the Boltzmann constant, T_g is the gas kinetic temperature, m is the mass of the molecule, and v_{turb} is the characteristic turbulent velocity in the cloud.

The System of Statistical Equilibrium Equations for the Level Populations

In the stationary case, the system of equations for the level populations is

$$\begin{aligned}\sum_{k=1, k \neq i}^M (R_{ki}(z) + C_{ki}) n_k(z) - n_i(z) \sum_{k=1, k \neq i}^M (R_{ik}(z) + C_{ik}) &= 0, \quad i = 1, \dots, M-1, \\ \sum_{i=1}^M n_i(z) &= 1,\end{aligned}\tag{5}$$

where M is the total number of levels, $R_{ik}(z)$ is the rate coefficient for the transition from level i to level k through radiative processes, and C_{ik} is the rate coefficient for the transition from level i to level k through collisional processes. The rate coefficients for radiative transitions $R_{ik}(z)$ are

$$\begin{aligned}R_{ik}^\downarrow(z) &= B_{ik} J_{ik}(z) + A_{ik}, \quad \varepsilon_i > \varepsilon_k, \\ R_{ik}^\uparrow(z) &= B_{ik} J_{ik}(z), \quad \varepsilon_i < \varepsilon_k.\end{aligned}$$

Here, A_{ik} and B_{ik} are the Einstein coefficients for spontaneous and stimulated emission, respectively; $J_{ik}(z)$ is the radiation intensity averaged over the direction and over the line profile:

$$J_{ik}(z) = \frac{1}{2} \int_{-\infty}^{\infty} d\nu \phi_{ik}(\nu) \int_{-1}^1 d\mu I(z, \mu, \nu),$$

where $I(z, \mu, \nu)$ is the solution of Eq. (4).

The collisional transitions of H₂O molecules in collisions with H and He atoms and H₂ molecules are considered in the model. If the level structure of the collisional partners is unimportant or if the

level populations have the Boltzmann distribution, then the principle of detailed balance holds for the molecule’s collisional excitation and de-excitation rate coefficients:

$$C_{ik} = \frac{g_k}{g_i} C_{ki} \exp\left(\frac{\varepsilon_i - \varepsilon_k}{kT_g}\right),$$

where the first index in the collisional rate coefficient denotes the initial level. In the case of a non-equilibrium level population distribution for the collisional partner, the rate coefficients for the collisional transitions of the H₂O molecule can be written as

$$C_{ik} = \sum_l \xi_l \sum_m C_{ik}^{lm}$$

where C_{ik}^{lm} is the rate coefficient for the transition of the H₂O molecule from level i to level k and the transition of the incident particle from level l to level m during the collision, ξ_l are the normalized level populations of the incident particle. The state-to-state rate coefficients C_{ik}^{lm} obey the principle of detailed balance:

$$C_{ik}^{lm} = \frac{g_k}{g_i} \frac{g_m}{g_l} C_{ki}^{ml} \exp\left(\frac{\varepsilon_i + \varepsilon_l - \varepsilon_k - \varepsilon_m}{kT_g}\right).$$

The sum $\sum_m C_{ik}^{lm}$ is called the effective collisional rate coefficient.

Collisional Rate Coefficients and Spectroscopic Data

In our calculations, we took into account 45 ortho-H₂O rotational levels and 9 H₂ rotational levels. The spectroscopic data for H₂O were taken from the HITRAN 2012 database (Rothman et al. 2013). The H₂ energy levels were taken from Dabrowski (1984).

We used the collisional rate coefficients for collisions between H₂O and H₂ molecules from Dubernet et al. (2009) and Daniel et al. (2010, 2011). In the calculations of these collisional rate coefficients, the interaction potential from Valiron et al. (2008) was used. The tables of rate coefficients are accessible in the BASECOL database¹ (Dubernet et al. 2006, 2013). Estimates of the effective collisional rate coefficients (summed over the final states of H₂) for H₂O de-excitation transitions for collisions with H₂ molecules in the states up to $J = 8$ are presented in the mentioned papers. We estimated the effective collisional rate coefficients for ortho-H₂O excitation (reverse) transitions in collisions with para-H₂ molecules based on data from Dubernet et al. (2009). The ortho-H₂ level populations in our calculations corresponded to the Boltzmann distribution. Therefore, the total rate coefficients for ortho-H₂O excitation (reverse) transitions for collisions with ortho-H₂ molecules were calculated from the principle of detailed balance.

The collisional rate coefficients for transitions between H₂O levels in inelastic collisions of H₂O with He atoms were taken from Green et al. (1993). The rate coefficients for transitions between H₂O levels in collisions of H₂O with H atoms were assumed to be a factor of 1.2 larger than those for collisions of H₂O with He atoms. The numerical coefficient allows for the difference in H and He atom masses and cross sections.

The Dust Model

In our calculations, we used the dust model from Weingartner and Draine (2001) and Draine (2003)². The dust emissivity was calculated in accordance with Kirchhoff’s radiation law. At dust temperatures $T_d \lesssim 100$ K, the dust radiation has virtually no effect on the H₂O level populations (Yates et al. 1997). Here, we did not consider the thermal balance of dust and gas.

¹<http://basecol.obspm.fr/>

²<http://www.astro.princeton.edu/~draine/dust/dustmix.html>

Numerical Calculations

The radiative transfer equation in the medium (4) and the statistical equilibrium equations for the molecular level populations (5) are a system of non-linear equations for the level populations of the H₂O molecule. This system of equations was solved by the accelerated Λ -iteration method (Rybicki and Hummer 1991).

The cloud in our numerical model was broken down into layers parallel to the cloud plane. The molecular level populations within each layer were constant. The thickness of the near-surface layer was chosen in such a way that the optical depth for any H₂O line and any considered direction in the layer was less than 1. The thickness of each succeeding layer into the cloud was larger than that of the preceding one by a constant factor. The number of layers into which the cloud was broken down is 100. The number of unknown molecular level populations is $N \times M$, where N is the number of cloud layers and M is the number of molecular levels. The range of values for the parameter μ is $[0; 1]$; the discretization step was chosen in our calculations to be 0.1. The deviation of the radiation frequency from the transition frequency is characterized by the parameter $x = (\nu - \nu_{ik})/\Delta\nu_{ik}$. The range of values for the parameter x for each line was chosen to be $[-5; 5]$; the discretization step is 0.25.

An additional acceleration of the iterative series was achieved by applying the convergence optimization method proposed by Ng (1974). The convergence criterion for the iterative series was the condition on the maximum relative increment in level populations for two successive iterations, $\max_i |\Delta n_i/n_i| < 10^{-4}$. In our calculations, we used the algorithms for solving systems of linear equations published in Rybicki and Hummer (1991) and in the book by Press et al. (1997). For a description of our calculations, see also Nesterenok (2013).

The calculations were performed on the supercomputer of the St. Petersburg branch of the Joint Supercomputer Center, the Russian Academy of Sciences.

Results

Ortho-H₂O Level Population Inversion in the 22.2-GHz Line

The population inversion for levels i and j is

$$\Delta n_{ij}(z) = \frac{n_i(z)}{g_i} - \frac{n_j(z)}{g_j},$$

where $\varepsilon_i > \varepsilon_j$. The cloud-averaged population inversion for levels i and j is calculated from the formula

$$\langle \Delta n_{ij} \rangle = \frac{1}{H} \int_0^H dz \Delta n_{ij}(z).$$

The excitation temperature T_{exc}^{ij} for two levels, i and j , is determined from the equality

$$\frac{1}{T_{\text{exc}}^{ij}} = \frac{k}{\Delta\varepsilon_{ij}} \ln \left(\frac{n_j g_i}{n_i g_j} \right),$$

where $\Delta\varepsilon_{ij} = \varepsilon_i - \varepsilon_j$, with $i > j$. For the H₂ $J = 0$ and 2 levels, $\Delta\varepsilon_{20} = 354.35 \text{ cm}^{-1}$. When the level excitation temperature T_{exc}^{ij} is equal to the gas temperature T_g , the level populations correspond to the Boltzmann distribution for a given temperature. If the lower-level population $n_j \rightarrow 0$, then $1/T_{\text{exc}}^{ij} \rightarrow -\infty$; for $n_i/g_i = n_j/g_j$, $1/T_{\text{exc}}^{ij} = 0$; when the upper-level population $n_i \rightarrow 0$, $1/T_{\text{exc}}^{ij} \rightarrow +\infty$.

Figure 2 presents the results of our calculations of the ortho-H₂O 6₁₆ and 5₂₃ level population inversion (the 22.2-GHz line) as a function of distance into the cloud. The results of our calculations are presented for a gas temperature of 400 K. The H₂ level populations correspond to the Boltzmann distribution

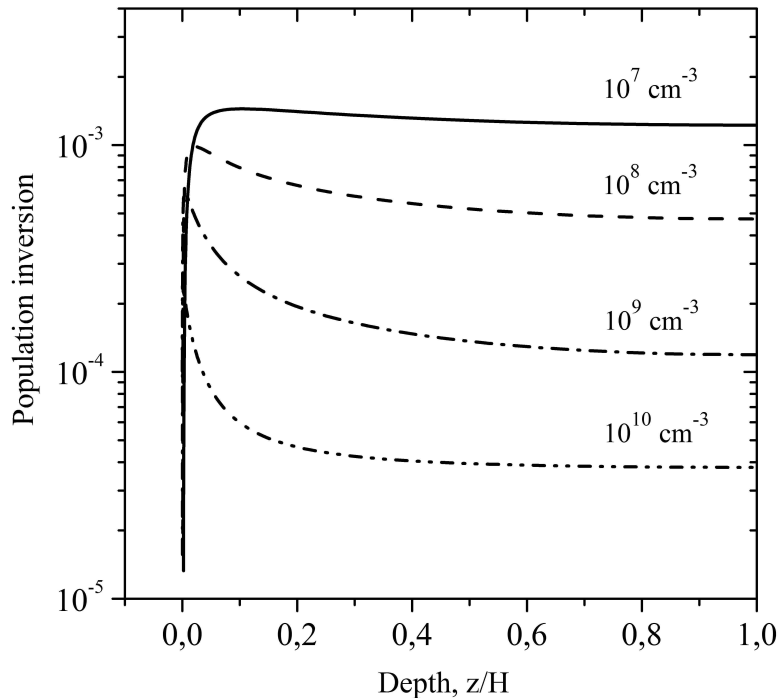


Figure 2: Ortho-H₂O 6₁₆ and 5₂₃ level population inversion (the 22.2-GHz line) versus distance into the cloud. The total number density of hydrogen atoms $N_{\text{H,tot}}$ is specified near each curve. The results of our calculations are presented for the gas temperature $T_g = 400$ K.

in this case. For distances $z/H \gtrsim 0.2$ into the cloud, the population inversion depends weakly on the coordinates. There is collisional maser pumping, with the sink line photons being absorbed by cold dust.

The H₂ $J = 0$ and 2 level populations were varied in our calculations, with their sum having remained fixed and equal to the sum of the populations for the Boltzmann distribution. The populations of the remaining H₂ levels corresponded to the Boltzmann distribution. The H₂ level populations were assumed to be independent of the z coordinate. For each distribution of H₂ level populations, i.e., for a fixed excitation temperature T_{exc}^{20} for the $J = 0$ and 2 levels, we solved the system of non-linear equations (4) and (5) for the ortho-H₂O level populations. The H₂O level populations are functions of the parameter T_{exc}^{20} .

Figure 3 presents the results of our calculations of the cloud-averaged ortho-H₂O level population inversion $\langle \Delta n_{ij} \rangle$ for the 22.2-GHz transition. The results were normalized to the parameter $\langle \Delta n_{ij} \rangle$ for a thermodynamically equilibrium H₂ level population distribution ($T_{\text{exc}}^{20} = T_g$). For gas densities $N_{\text{H,tot}} \lesssim 10^8 \text{ cm}^{-3}$, the 6₁₆ and 5₂₃ level population inversion increases with increasing H₂ $J = 2$ level population. Thus, the effect of quasi-resonance energy transfer in collisions between H₂O and H₂ leads to more efficient H₂O maser pumping. For high gas densities $N_{\text{H,tot}} \gtrsim 10^9 \text{ cm}^{-3}$, this effect has the opposite sign. The effect of quasi-resonance energy transfer in collisions between H₂O and H₂ weakens with increasing gas temperature.

Ortho-H₂O Level Population Inversion in the 380-, 439-, and 621-GHz Lines

The 380-, 439-, and 621-GHz lines correspond to the ortho-H₂O 4₁₄ → 3₂₁, 6₄₃ → 5₅₀, and 5₃₂ → 4₄₁ transitions, respectively. The maser emission in the 439- and 621-GHz lines was observed in the envelopes

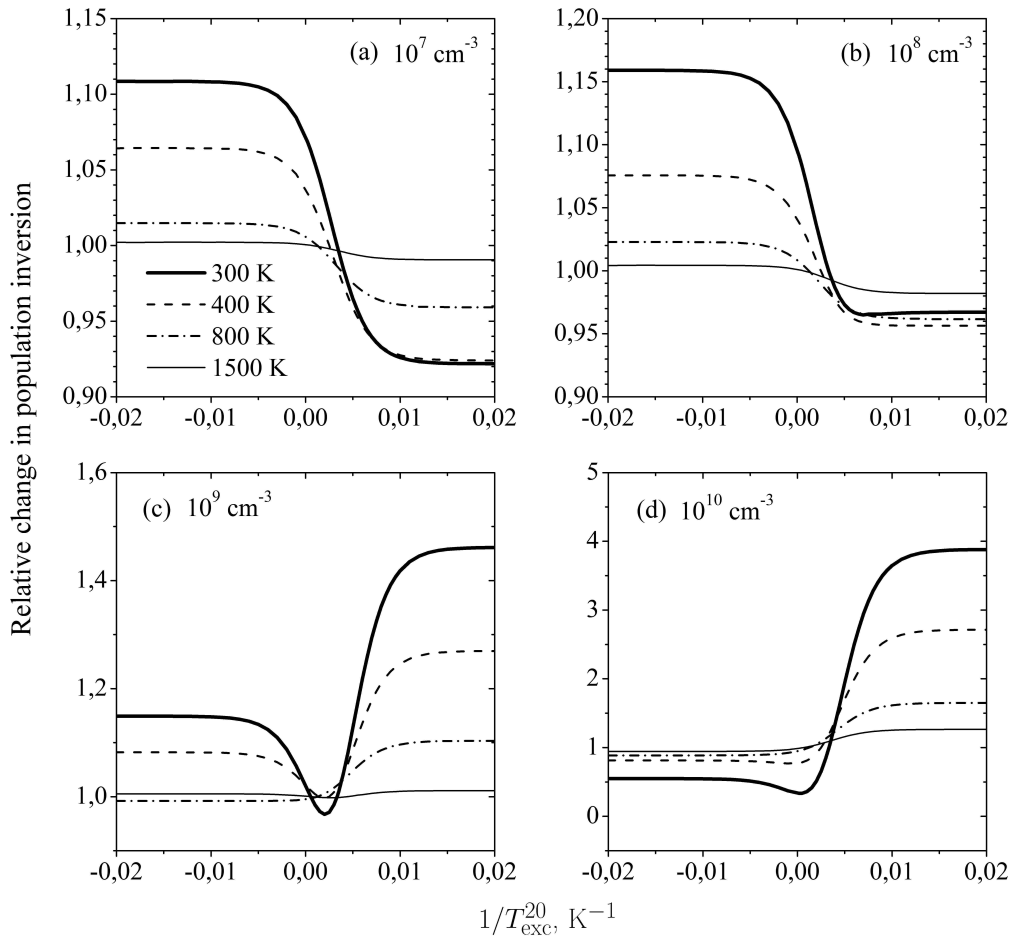


Figure 3: Relative change in ortho- H_2O 6_{16} and 5_{23} level population inversion (the 22.2-GHz line) $\langle \Delta n_{ij} \rangle / \langle \Delta n_{ij}(T_g) \rangle$ is along the vertical axis, where $\langle \Delta n_{ij}(T_g) \rangle$ is the value of the parameter in the case of a thermodynamically equilibrium H_2 level population distribution. The parameter $1/T_{\text{exc}}^{20}$ is along the horizontal axis, where T_{exc}^{20} is the excitation temperature of the H_2 $J = 0$ and 2 levels. The total number density of hydrogen atoms $N_{\text{H,tot}}$ is specified on each plot.

of late-type stars and in star-forming regions in our Galaxy (Melnick et al. 1993; Neufeld et al. 2013). The 439-GHz line was also observed toward the galaxy NGC 3079 (Humphreys et al. 2005).

Figure 4 presents the results of our calculations of the cloud-averaged H_2O level population inversion $\langle \Delta n_{ij} \rangle$ for the 380-, 439-, and 621-GHz transitions. The results of our calculations are presented for the gas number densities $N_{\text{H,tot}} = 10^8 \text{ cm}^{-3}$, and 10^9 cm^{-3} . For some values of the physical parameters, the level population inversion exists only at $1/T_{\text{exc}}^{20}$ below some critical value (i.e., for high H_2 $J = 2$ level population). Thus, there is quasi-resonance H_2O maser pumping.

The H_2O level population inversion is proportional to the fraction of H_2 molecules at excited levels. For the gas temperature $T_g = 400 \text{ K}$ and under the condition $1/T_{\text{exc}}^{20} \rightarrow -\infty$, the H_2 $J = 2$ level population in our model is 0.2 (in this case, the $J = 0$ level population is 0). The level population inversion is also proportional to the number of quasi-resonance H_2O transitions involved in the maser pumping. The number of such transitions in our model is about 10-30 for the maser lines under consideration.

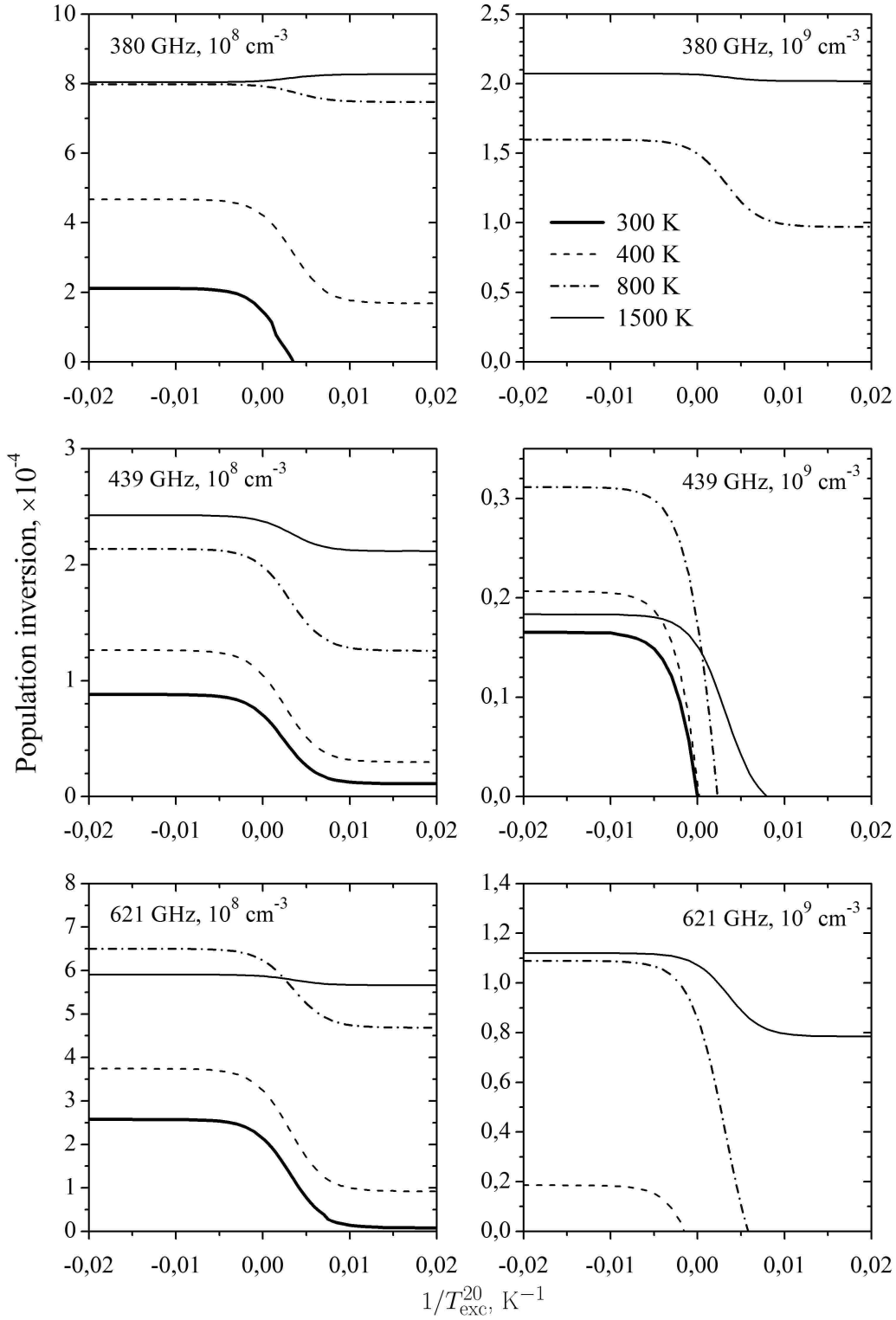


Figure 4: Ortho- H_2O 4_{14} and 3_{21} (the 380-GHz line), 6_{43} and 5_{50} (the 439-GHz line), 5_{32} and 4_{41} (the 621-GHz line) level population inversion versus parameter $1/T_{\text{exc}}^{20}$. The transition frequency and the total number density of hydrogen atoms $N_{\text{H,tot}}$ are specified on each plot.

Discussion

The turbulent motions of gas in molecular clouds, the expansion of compact HII regions, and the interaction of bipolar outflows from protostars and young stars with clouds of molecular gas give rise to shock waves. The possibility of the generation of intense H₂O maser emission in shocks in star-forming regions was considered in Strel'nitskii (1973), Elitzur et al. (1989), Hollenbach et al. (2013), and other papers. In dissociative shocks, there is collisional dissociation of H₂ molecules in a hot gas at the shock front (Flower 2007). As the distance from the shock front increases, the gas temperature decreases and H₂ molecules are formed on dust particles. The gas temperature in this region of the molecular flow is 300-400 K and the generation of H₂O maser emission is possible (Hollenbach et al. 2013). The H₂ molecules formed on dust particles are at excited rotational-vibrational levels and there can be quasi-resonance energy transfer in collisions between H₂ and H₂O molecules.

The central engines of AGNs are powerful sources of X-ray emission. Because of the high photon energy and the small absorption cross section, the X-ray emission exerts a deeply penetrating action on the physical properties of the interstellar medium (Malony et al. 1996). To all appearances, the H₂O maser emission in the central regions of AGNs is generated in clouds of gas and dust, in which the physical conditions are governed by the X-ray emission from the central engine, i.e., in X-ray dissociation regions (Neufeld et al. 1994; Collison and Watson 1995; Malony 2002). In X-ray dissociation regions, the interaction of high-energy photoelectrons with atoms and molecules of the gas leads to the excitation of electronic and vibrational states of molecules. In addition, the H₂ molecules formed on dust particles are at highly excited rotational-vibrational levels.

One of the main mechanisms for the excitation of high-energy rotational-vibrational H₂ levels is the formation of molecules on dust particles. For gas number densities $N_{\text{H,tot}} \gtrsim 10^5 \text{ cm}^{-3}$, the de-excitation of excited H₂ levels occurs through collisions with H atoms, provided that $N_{\text{H}} \sim N_{\text{H}_2}$ (Hollenbach and Tielens 1999). Let n_x be the fraction of H₂ molecules at highly excited rotational-vibrational levels. In the stationary case, the excitation rate of high-energy molecular levels is equal to the de-excitation rate. We can then write

$$R_{\text{gr}} N_{\text{H,tot}} N_{\text{H}} = C_x n_x N_{\text{H}_2} N_{\text{H}}, \quad (6)$$

where R_{gr} is the specific formation rate of H₂ molecules on dust and C_x is the mean collisional de-excitation rate of excited H₂ levels. For our estimates, we take R_{gr} to be $3 \times 10^{-17} \text{ cm}^3 \text{ s}^{-1}$ (Bourlot et al. 2012). Assuming that the H₂ molecule is de-excited after 3-5 collisions and that $T_g = 400 \text{ K}$, we have an estimate of $\sim 10^{-11} \text{ cm}^3 \text{ s}^{-1}$ for C_x (Wrathmall et al. 2007). From Eq. (6) we have

$$n_x \simeq 10^{-5} \left(\frac{0.3}{x_{\text{H}_2}} \right),$$

where $x_{\text{H}_2} = N_{\text{H}_2}/N_{\text{H,tot}}$. The number of H₂O and H₂ transitions for which the quasi-resonance conditions are met and which can be involved in the H₂O maser pumping is $10^4 - 10^5$. When estimating this number, we took into account 318 H₂ rotational-vibrational levels and the possibility of H₂O vibrational state excitation. A large number of quasi-resonance transitions can lead to a noticeable effect, despite the relatively small fraction of H₂ molecules in highly excited states.

Conclusions

We considered the effect of quasi-resonance energy transfer in collisions between H₂ and H₂O molecules on the H₂O maser pumping process. We calculated the populations of 45 ortho-H₂O rotational levels for various populations of the para-H₂ $J = 0$ and 2 rotational levels. The H₂O level population inversion in the 22.2-, 380-, 439-, and 621-GHz maser lines was shown to depend significantly on the population

distribution of the lower H₂ rotational levels. For some of the physical parameters, the effect of quasi-resonance energy transfer between molecules leads to a high H₂O level population inversion in lines of the submillimeter wavelength range; while the H₂O level population inversion in the model with a thermodynamically equilibrium H₂ level population distribution is either small or absent. The quasi-resonance energy transfer effect can play a significant role in pumping H₂O masers in the central regions of AGNs and in star-forming regions.

Acknowledgements

This work was supported in part by the Russian Foundation for Basic Research (project no. 14-02-31302), the Program of the President of Russia for Support of Leading Scientific Schools (project no. NSh-294.2014.2), and the Research Program OFN-17, the Division of Physics of the Russian Academy of Sciences.

References

1. Babkovskaia N. and Poutanen J., *Astron. Astrophys.* **418**, 117 (2004).
2. Bolgova G.T., Strel'nitskii V.S., Shmeld I.K., *Soviet Astronomy* **21**, 468 (1977).
3. Castangia P., Impellizzeri C.M.V., McKean J.P., Henkel C., Brunthaler A., Roy A.L., Wucknitz O., Ott J., et al., *Astron. Astrophys.* **529**, A150 (2011).
4. Churchwell E., Witzel A., Huchtmeier W., Pauliny-Toth I., Roland J., and Sieber W., *Astron. Astrophys.* **54**, 969 (1977).
5. Collison A.J. and Watson W.D., *Astrophys. J.* **452**, L103 (1995).
6. Dabrowski I., *Canad. J. Phys.* **62**, 1639 (1984).
7. Daniel F., Dubernet M.-L., Pacaud F., and Grosjean A., *Astron. Astrophys.* **517**, A13 (2010).
8. Daniel F., Dubernet M.-L., and Grosjean A., *Astron. Astrophys.* **536**, A76 (2011).
9. dos Santos P.M. and Lépine J.R.D., *Nature* **278**, 34 (1979).
10. Draine B.T., *Ann. Rev. Astron. Astrophys.* **41**, 241 (2003).
11. Dubernet M.-L., Grosjean A., Flower D., Roueff E., Daniel F., Moreau N., and Debray B., *J. Plasma Fusion Res. Series* **7**, 356 (2006).
12. Dubernet M.-L., Daniel F., Grosjean A., and Lin C.Y., *Astron. Astrophys.* **497**, 911 (2009).
13. Dubernet M.-L., Alexander M.H., Ba Y.A., Balakrishnan N., Balança C., Ceccarelli C., Cernicharo J., Daniel F., et al., *Astron. Astrophys.* **553**, A50 (2013).
14. Elitzur M., Hollenbach D.J., and McKee C.F., *Astrophys. J.* **346**, 983 (1989).
15. Flower D.R., *Molecular collisions in the interstellar medium* (New York: Cambridge University Press, 2007).
16. Green S., Maluendes S., and McLean A.D., *Astrophys. J. Suppl. Ser.* **85**, 181 (1993).
17. Greenhill L.J., Booth R.S., Ellingsen S.P., Herrnstein J.R., Jauncey D.L., McCulloch P.M., Moran J.M., Norris R.P., et al., *Astrophys. J.* **590**, 162 (2003).
18. Hollenbach D.J. and Tielens A.G.G.M., *Reviews of Modern Physics* **71**, 173 (1999).
19. Hollenbach D., Elitzur M., and McKee C.F., *Astrophys. J.* **773**, 70 (2013).
20. Humphreys E.M.L., Greenhill L.J., Reid M.J., Beuther H., Moran J.M., Gurwell M., Wilner D.J., and Kondratko P.T., *Astrophys. J.* **634**, L133 (2005).
21. Kartje J.F., Königl A., and Elitzur M., *Astrophys. J.* **513**, 180 (1999).
22. Le Bourlot J., Le Petit F., Pinto C., Roueff E., and Roy F., *Astron. Astrophys.* **541**, A76 (2012).
23. Liljeström T., Mattila K., Toriseva M., and Anttila R., *Astron. Astrophys. Suppl. Ser.* **79**, 19 (1989).
24. Maloney P.R., Hollenbach D.J., and Tielens A.G.G.M., *Astrophys. J.* **466**, 561 (1996).
25. Maloney P.R., *Publ. Astron. Soc. Aust.* **19**, 401 (2002).

26. Matveenko L.I., Diamond P.J., Graham D.A., *Astronomy Reports* **44**, 592 (2000).
27. Matveenko L.I., Demichev V.A., *Astronomy Reports* **54**, 986 (2010).
28. Melnick G.J., Menten K.M., Phillips T.G., and Hunter T., *Astrophys. J.* **416**, L37 (1993).
29. Moran J.M., *Frontiers of Astrophysics: A Celebration of NRAO's 50th Anniversary*, ASP Conference Series 395 (Ed. Bridle A.H., Condon J.J., and Hunt G.C., Charlottesville, 2008), p.87.
30. Nesterenok A.V., Varshalovich D.A., *Astronomy Letters* **37**, 456 (2011).
31. Nesterenok A.V., *Astronomy Letters* **39**, 717 (2013).
32. Neufeld D.A., Maloney P.R., and Conger S., *Astrophys. J.* **436**, L127 (1994).
33. Neufeld D.A., Wu Y., Kraus A., Menten K.M., Tolls V., Melnick G.J., and Nagy Z., *Astrophys. J.* **769**, 48 (2013).
34. Ng K.-C., *J. Chem. Phys.* **61**, 2680 (1974).
35. Palagi F., Cesaroni R., Comoretto G., Felli M., and Natale V., *Astron. Astrophys. Suppl. Ser.* **101**, 153 (1993).
36. Peck A.B., Henkel C., Ulvestad J.S., Brunthaler A., Falcke H., Elitzur M., Menten K.M., and Gallimore J.F., *Astrophys. J.* **590**, 149 (2003).
37. Press W.H., Teukolsky S.A., Vetterling W.T., and Flannery B.P., *Numerical Recipes in C. The Art of Scientific Computing* (Cambridge: Cambridge Univ. Press, 1997).
38. Rothman L.S., Gordon I.E., Babikov Y., Barbe A., Chris Benner D., Bernath P.F., Birk M., Bizzocchi L., et al., *J. Quant. Spectrosc. Rad. Transfer* **130**, 4 (2013).
39. Rybicki G.B. and Hummer D.G., *Astron. Astrophys.* **245**, 171 (1991).
40. Strel'nitskii V.S., *Sov. Astron.* **17**, 717 (1973).
41. Tarchi A., *Cosmic Masers - from OH to H₀*, *Proceedings IAU Symposium* **287**, 323 (2012).
42. Tennyson J., Zobov N.F., Williamson R., and Polyansky O.L., *J. of Physical and Chemical Reference Data* **30**, 735 (2001).
43. Torrelles J.M., Patel N., Gómez J.F., Anglada G., and Uscanga L., *Astrophys. Space Sci.* **295**, 53 (2005).
44. Uscanga L., Cantó J., Curiel S., Anglada G., Torrelles J.M., Patel N.A., Gómez J.F., and Raga A.C., *Astrophys. J.* **634**, 468 (2005).
45. Valiron P., Wernli M., Faure A., Wiesenfeld L., Rist C., Kedžuch S., and Noga J., *J. Chem. Phys.* **129**, 134306 (2008).
46. Varshalovich D.A., Kegel W.K., Chandra S., *Soviet Astronomy Letters* **9**, 209 (1983).
47. Weingartner J.C. and Draine B.T., *Astrophys. J.* **548**, 296 (2001).
48. Wrathmall S.A., Gusdorf A., and Flower D.R., *Mon. Not. R. Astron. Soc.* **382**, 133 (2007).
49. Yates J.A., Field D., and Gray M.D., *Mon. Not. R. Astron. Soc.* **285**, 303 (1997).